View metadata, citation and similar papers at core.ac.uk
brought to you by CORE
provided by Okayama University Scientific Achievement Repository

Development of an evaluation tool for a driving seat reducing neck injury based on mechanical impedance

Shunsuke Fukushima*, Yuhei Nomoto*, Yoshiyuki Tanaka*,
Toshio Tsuji*, Toru Takeshima**, Masaya Yamashita**
*Graduate school of engineering, Hiroshima University
1-4-1 Kagamiyama, Higashi-hiroshima, Hiroshima, Japan
fukushima@bsys.hiroshima-u.ac.jp
**DELTA KOGYO CO.,LTD.
1-14 Futyu-cho, Aki-gun, Hiroshima, Japan

***Abstract*—The importance of developing a driving seat effective for reducing neck injuries caused by rear-end collisions has been increased to produce a safer automobile against vehicle accidents in recent years. The present paper develops a computer simulator based on a mechanical impedance model for analyzing and designing an effective driving seat reducing neck injuries. The simulator can reproduce dynamic behaviors of a dummy doll measured in an actual test of rear-end collision. Effectiveness of an active headrest, which is developed for reducing neck injuries, is quantitatively evaluated through a set of computer simulations.**

I. Introduction

Rear-end accidents occupy about 30 % of the vehicle accidents (about 800 thousands) occurred in Japan in 2007 [1], and about 45 % victims of rear-end accidents suffer from whiplash injuries and spinal cord injuries, so-called Neck Injuries [2]. Accordingly, the driving seat effective for reducing neck injuries will be more important to produce a safer automobile in the near future.

There have been many studies concerned with neck injuries. For example, Svensson et al. [3] examined the mechanism of neck injuries through the experiments with a pig instead of a human driver, and reported that the change of pressure in the spinal column would be a main factor causing neck injuries. Some experimental researches using a living human as well as a cadaver presented a quantitative evaluation index for neck injuries. Boström et al. [4] proposed the neck injury criteria (NIC) which evaluates the relative acceleration and velocity between the head and the 1st thoracic vertebrae. Schmitt et al. [5] proposed the neck protection criteria (Nkm) which evaluates the shear force and the sagittal bending moment of the neck. Svensson et al. [6] and Nilson [7] produced a prototype seat against neck injuries, in which the headrest and the seatback was devised for reducing neck injuries, and reported that the degree of neck injuries becomes larger as the stiffness of a seatback joint increases through the vehicle collision test in rear-end impacts with a dummy doll. They also pointed out that the force transfer characteristics between a human driver and a seat are important to discuss the mechanism of neck injuries.

On the other hand, several studies have tried to reveal the neck injury mechanism by means of computer simulation techniques. Furusu [8] created a model of the human cervical vertebrae by the finite element method (FEM) and examined the correlation between the injury to the cervical vertebrae and the shear force along the sagittal axis of the cervical vertebrae. Also, Kirkpatrick et al. [9] constructed a computer model of a human driver by using LS-DYNA, which is the multi purpose analyzer tool based on the FEM, and simulated various situations of the vehicle collision. Huang et al. [10][11] created the model of a human and a seat by the FEM, and investigated human dynamic behaviors according to the seatback joint angle, and the influence on the cervical part according to the headrest position. The FEM model, however, requires a long time and many parameters in analysis, although the FEM model enables to detail analysis.

Our research group has proposed the analysis and design method of a driving seat for reducing neck injuries based on mechanical impedance with multi-body dynamics [12]. This can be much expected to shorten time in analysis than the FEM model. However, the values of impedance parameters in the developed model were inadequate and the actual shapes of human and seat were not considered.

This study develops a human-seat model to realize more advanced analysis of neck injuries by newly considering the nonlinear dynamic characteristics of seat and the real surface shapes of human and seat. This paper is organized as follows: Section 2 explains the neck injury analyzer tool composed of human-seat model based on multi-body dynamics, and describes the impedance estimation method of a seat surface and shows estimated results. Section 3 performs the simulation of human dynamic behaviors in rear-end accidents, and verifies both effectiveness of the proposed model and effectiveness of an active headrest developed for reducing neck injuries.

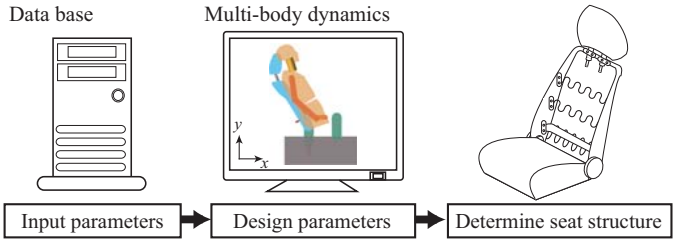

Fig. 1. Design process using the simulation system.

II. The neck injury analyzer tool

A. System structure

Figure 1 shows the general design process of a driving seat against neck injuries by the developed analyzer. The system has a database of the physical parameters of a human-seat model such as the stature and weight of a human driver, the size and weight of seat parts, and the impedance properties of driver's skin and joints, which had been measured or estimated in advance. A dummy doll is used instead of a human driver in this paper.

This tool can simulate dynamic behaviors of human-seat model in rear-end impacts, and can evaluate the degree of neck injuries according to the viscoelastic properties of seat surface and joint.

B. Dynamic model of the human-seat

Figure 2 (a) shows a schematic representation of the human-seat model. Dynamic characteristics of human and seat are modeled by a mechanical impedance model. To simplify the discussion, the human model is composed of a head, a torso, and arms, while the seat model is composed of a headrest and a seatback. The human model is expressed by 14 rigid links with 14 DOFs, which has 2 prismatic joints and 12 rotational joints (h_1: the hip joint, h_2: the 5th lumbar vertebrae joint, h_3: the 1st lumbar vertebrae joint, h_4: the 7th cervical vertebrae joint, h_5: the 1st cervical vertebrae joint, and 6 joints for the vertebral disks, h_6: the shoulder joint). Note that the neck is expressed with a beam model based on the Timoshenko beam theory [13]. The seat model is expressed by 4 rigid links with 4 DOFs, which has one prismatic joint and 3 rotational joints (s_1: the joint between bearing surface and seatback, s_2: the joint in the active headrest mechanism, s_3: the joint between seatback and headrest). The human-seat rigid links have real surface shapes of human and seat.

Generally, the dynamic equation of a rigid model with n links in the 2-dimensional space can be written as

$$M_{q_i}\ddot{q}_i + h(q_i, \dot{q}_i) + g(q_i) + B_{q_i}\dot{q}_i + K_{q_i}(q_i - q_{v_i}) = \tau_{ext_i}, \quad (1)$$

where $q_i \in \Re^n$ ($i \in h$: human, s: seat) represents the vector of joint angle/translational position, and q_{v_i} represents the virtual equilibrium angle/position for the stiffness. $M_{q_i}, B_{q_i}, K_{q_i} \in \Re^{n\times n}$ represent the inertia, viscosity, and stiffness matrices, respectively; $h(q_i, \dot{q}_i) \in \Re^n$ refers to the centrifugal and coriolis forces; $g(q_i) \in \Re^n$ relates to the gravity force; and $\tau_{ext_i} \in \Re^n$ is the external force. As shown in Fig. 2 (a), the

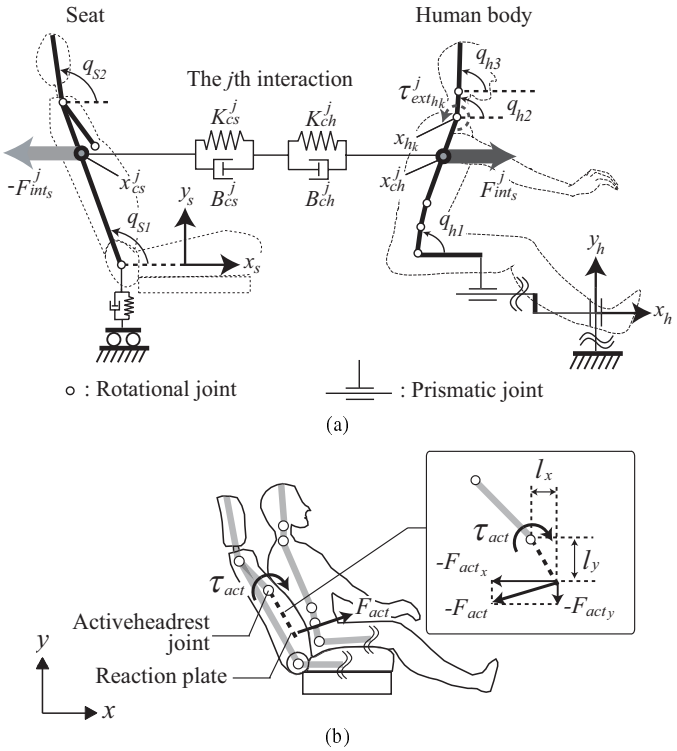

Fig. 2. A schematic description of the human-seat model using mechanical impedance.

external force τ_{ext_i} is caused by vertical interaction forces, $F^j_{int_i} \in \Re^2$ ($j = 1, \ldots, M$), at M contact points between the human and the seat. The interaction force $F^j_{int_s}$ applied from the seat to the human at a contact point is given as follows:

$$F^j_{int_s} = f^j_{int_s}\frac{x^j_{ch} - x^j_{cs}}{x^j_c}, \quad (2)$$

$$f^j_{int_s} = \begin{cases} -B^j_{cs}\dot{x}^j_c - K^j_{cs}(x^j_c - x^j_{cv}) \\ \qquad (x^j_c - x^j_{cv} < -d^j_{skin}) \\ -(\frac{B^j_{cs}B^j_{ch}}{B^j_{cs}+B^j_{ch}})\dot{x}^j_c - (\frac{K^j_{cs}K^j_{ch}}{K^j_{cs}+K^j_{ch}})(x^j_c - x^j_{cv}) \\ \qquad (-d^j_{skin} \le x^j_c - x^j_{cv} \le 0) \\ 0 \qquad (x^j_c - x^j_{cv} > 0), \end{cases} \quad (3)$$

where $B^j_{ci}, K^j_{ci} \in \Re^1$ ($i = h, s$) indicate the surface viscosity and stiffness at the contact point j, respectively; x^j_c is the distance of the virtual contact points between the point on human rigid link $x^j_{ch} \in \Re^2$ and the point on seat's rigid link $x^j_{cs} \in \Re^2$; x^j_{cv} shows the equilibrium position for K^j_{ci}; and d^j_{skin} is the thickness of the skin.

In the automotive industry, development of an active headrest mechanism has been accelerated to achieve the goal of reducing neck injuries in vehicular rear-end accidents. The active headrest is a mechanism which easily holds up the head and reduces neck injuries by moving the headrest forward. In the seat used for a rear-end impact test, the headrest is moved forward by the torque τ_{act} applied from the interaction force F_{act} between the lower torso and the reaction plate in the

seatback by [14]

$$\tau_{act} = \begin{cases} -F_{act_x} l_y - F_{act_y} l_x & (F_{act} > F_{threshold}) \\ 0 & (F_{act} < F_{threshold}), \end{cases} \quad (4)$$

where $F_{threshold}$ is the force necessary to activate the headrest, and l is the distance between the reaction plate and the active headrest joint (See Fig. 2 (b)).

C. Viscoelastic properties of a driving seat

Dynamics of the seat surface to a normal force $dF_{cs}(t)$ can be expressed by

$$B_{cs}(dX)d\dot{X}(t) + K_{cs}(dX)dX(t) = -dF_{cs}(t), \quad (5)$$

where $dX(t)$ denotes the displacement of a seat surface from onset time; $B_{cs}(dX)$ and $K_{cs}(dX)$ represent the seat viscosity and stiffness parameters. In this paper, such viscoelastic parameters of the seat were obtained by two experimental tests: a quasi-static loading test for estimating $K_{cs}(dX)$ (Fig. 3 (a)), and a dynamic loading test for estimating $B_{cs}(dX)$ (Fig. 3 (b)). Estimation points were set at the upper, middle, and lower parts on the halfway line of a seatback and the central part of a headrest as show in Fig. 3 (c).

In the quasi-static test, the rigid load deliberately presses the seat surface under $d\dot{X} \approx 0$ so that the viscous term in Eq. (5) can be omitted as

$$K_{cs}(dX)dX(t) = -dF_{cs}(t). \quad (6)$$

The stiffness $K_{cs}(dX)$ can be estimated by fitting the displacement dX and the external force dF_{cs} into Eq. (6).

In the dynamic loading test, a rigid load with a sufficient large mass M_0 falls freely and deforms the seat surface. The dynamic equation of the rigid load is then expressed as

$$F_{cs}(t) = M_0\ddot{X}(t) + M_0 g, \quad (7)$$

where $\ddot{X}(t)$ represents the acceleration of rigid load after the contact with seat surface. That is, the force applied to the seat by the rigid load F_{cs} can be calculated by Eq. (7). Accordingly, the viscosity $B_{cs}(dX)$ can be estimated by fitting the displacement dX and the calculated force dF_{cs} into Eq. (5) with the stiffness $K_{cs}(dX)$ that have already be estimated in the quasi-static loading test.

Figure 3 (a) shows a schematic diagram of the experimental set-up for the quasi-static loading test. The table on which the seat is fixed moves upwards toward the hemispheric rigid load (mass: 6.8 [kg], diameter: ϕ = 165 [mm]) attached to the tip of the spring (rate of spring k_{spring}: 3.1646 [kgf/mm]) at a constant speed of 4.5 [mm/s] to deform the seat surface by the rigid load. The displacement of the table and the spring (dX_{table} and dX_{spring}) is measured by a strain gauge displacement sensor (sampling frequency: 1 [kHz]) to calculate dX and dF_{cs} by

$$\begin{cases} dX(t) = dX_{table}(t) - dX_{spring}(t) \\ dF_{cs}(t) = k_{spring} dX_{spring}(t) \end{cases} \quad (8)$$

for estimating $K_{cs}(dX)$ with Eq. (6).

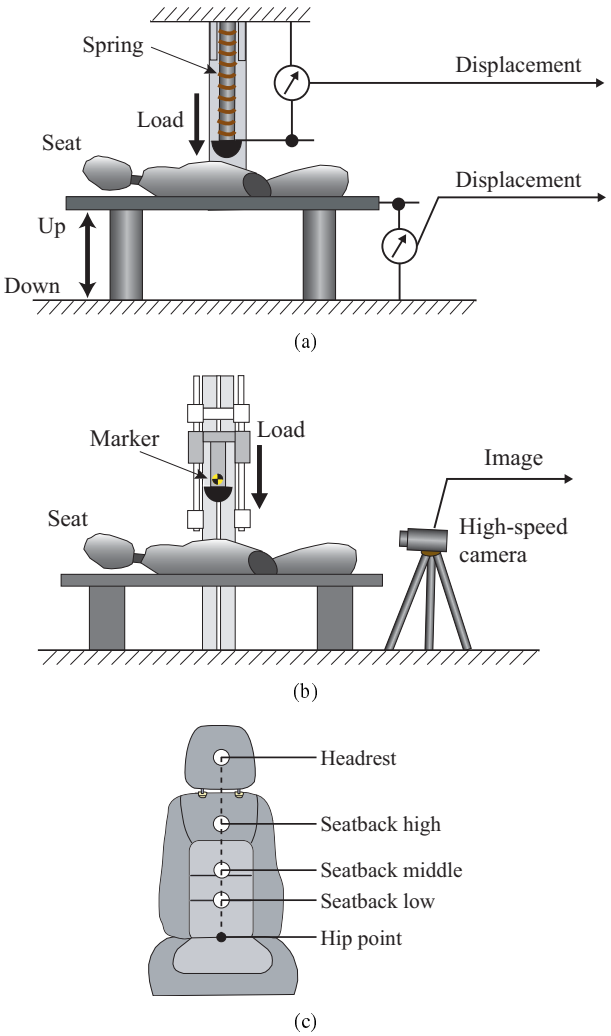

Fig. 3. Schematic illustration of the loading test for the seatback surface.

Figure 3 (b) shows a schematic illustration constructed for the dynamic loading test. The hemispheric rigid load (mass: 6.8 [kg], diameter: ϕ = 165 [mm]) is attached to the tip of the movable frame of the testing machine, and falls freely to the seat fixed to the table from 300 [mm] above. A marker on the rigid load is observed using a high-speed camera (sampling rate: 1 [kHz]) to measure the displacement of the seat surface dX during deformations.

Figures 4 (a) and (b) show the seat stiffness and viscosity estimated at the specified four points, respectively. The viscoelasticity was modeled by the following nonlinear polynomial expressions with respect to the displacement dX in this paper as

$$K_{cs}(dX) = \sum_{p=0}^{5} a_p dX^p, \quad B_{cs}(dX) = \sum_{q=0}^{5} b_q dX^q, \quad (9)$$

where the parameters a_p and b_q $(p = 0, 1, 2, \ldots, 5; q = 0, 1, 2, \ldots, 5)$ were determined by a non-linear fitting method with the measured data. It can be confirmed that viscoelastic characteristics of seat surface change non-linearly according to the displacement at all the measured points. These non-linear

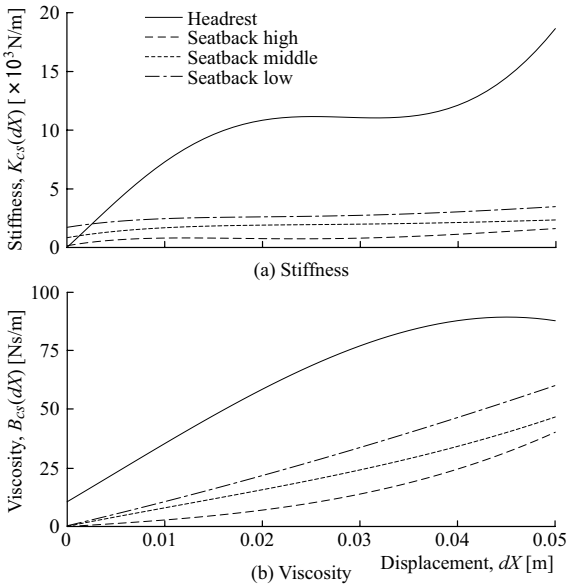

Fig. 4. Results of the viscoelastic properties estimated using the proposed method.

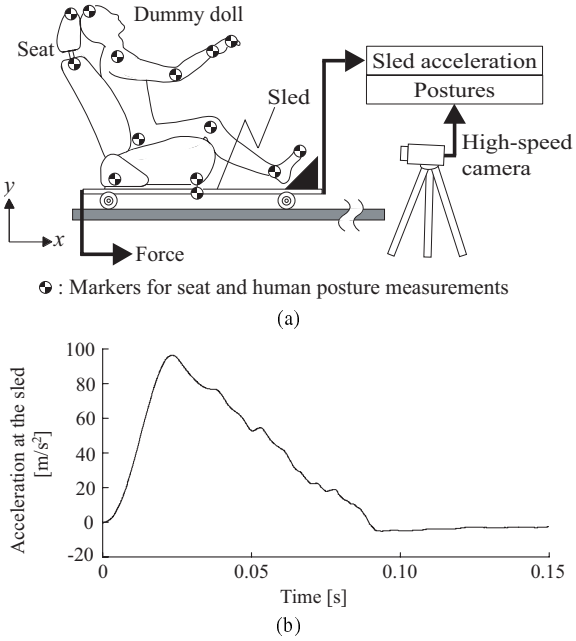

Fig. 5. Experimental apparatus and acceleration measured at the sled.

dynamic properties of an actual seat were installed into the human-seat model for the computer simulations.

III. Computer simulation with the proposed model

A. Rear-end impact testing

Figure 5 (a) shows a schematic drawing of the experimental apparatus. A seat with the active headrest mechanism and a dummy (BioRID-II, Denton ATD) are set on the sled of crash simulation system with 1 DOF (Instron Structural Testing Systems). Markers were attached at the joint positions of the seat and the dummy, and the posture of each was measured using Image Express Motion (Sensors Applications). This apparatus can reproduce the dynamic behaviors of seat and dummy in an actual rear-end accident.

In this experiment, the acceleration toward x-axis was measured using acceleration sensors attached to dummy and sled. Figure 5 (b) shows the time profile of the measured acceleration added to the sled.

From the accelerations of measured points, the NIC value can be calculated as [4]

$$\begin{cases} NIC(t) = 0.2a_{rel}(t) + (v_{rel}(t))^2 \\ a_{rel}(t) = a_{T_1}(t) - a_{head}(t) \\ v_{rel}(t) = v_{T_1}(t) - v_{head}(t) \end{cases} \tag{10}$$

where $a_{T_1}(t)$ and $a_{head}(t)$ represent the acceleration of the 1st thoracic vertebrae and the head in the x direction, respectively; $v_{T_1}(t)$ and $v_{head}(t)$ are the velocities of the 1st thoracic vertebrae and the head in the x direction, respectively; and $a_{rel}(t)$ and $v_{rel}(t)$ are the relative acceleration and velocity between the 1st thoracic vertebrae and the head. The load on the neck can be evaluated using the maximum value of NIC measuring in the test. The load on the neck is larger as the maximum NIC value is larger.

B. Computer simulation experiments

In the simulation, the joint position between a bearing surface and a seatback in the initial posture was set at the origin, and the acceleration toward x-axis measured in the rear-end impact testing was given against the carriage under the seatback as an input (See Fig. 5 (b)). Duration time of the simulations was 0.18 [s], and the sampling time for dynamic calculation was 0.0001 [s]. The viscoelasticity of a seat surface was set the parameter which was estimated by the method in previous section, and the stiffness and viscosity of human skin were set as K_{ch} = 366.00 [N/m], B_{ch} = 1.23 [Ns/m], respectively; and the thickness of human skin was at d_{skin} = 0.005 [m][15].

The rest 25 parameters were determined using an optimization technique of the Generalized Reduced Gradient Method [16]. The optimization function is defined by

$$Criterion = \sum_{i=1}^{N} c_i (Val^i_{mes} - Val^i_{sim})^2, \tag{11}$$

where Val^i_{mes} is the measurement data of the rear-end impact testing, Val^i_{sim} is the simulation data by the proposed model, and c_i is a weighting factor. This represents the error of behavior between a human-seat model in the simulation and a dummy-seat in the rear-impact testing.

Figure 6 shows the experimental and simulated dynamic behaviors of the human and the seat at 0.03, 0.09, and 0.15 [s] from the top to the below, and Fig. 7 shows the time histories of the headrest angle, the seatback angle, the head angle, the neck angle and torso angle. It is noted that each of the angles represents the angle from x-axis in the absolute coordinate system. The continuous line represents the simulation result and the broken line represents the result from the experiment, while the continuous line corresponds approximately to the

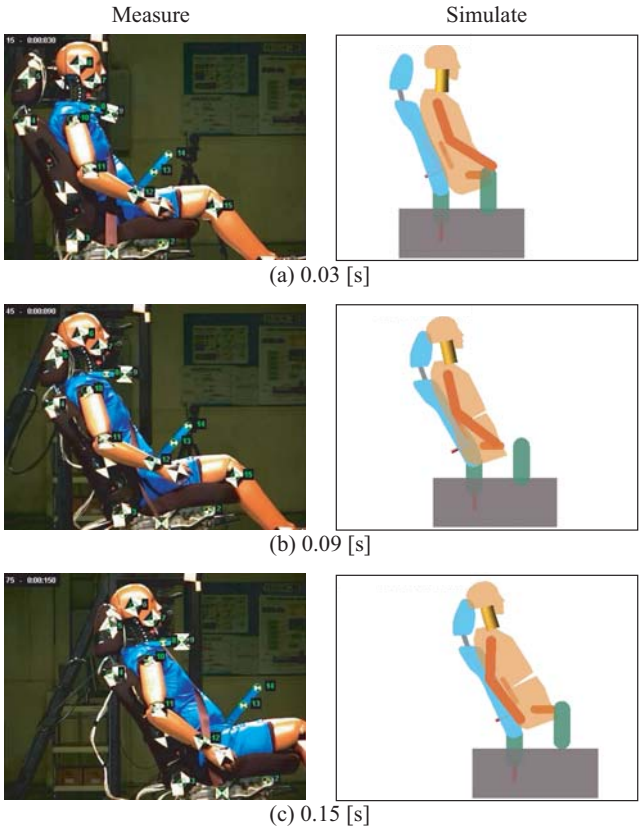

Fig. 6. Comparison of the experimental and simulated dynamic behaviors.

broken line. Figure 8 shows the time histories of NIC values and the acceleration of the 1st thoracic vertebrae and the head for both the rear-end impact tests and the simulations. The continuous line represents the simulation result and the broken line shows the experimental result, while the continuous line corresponds approximately to the broken line. These results demonstrate that the proposed model realistically recreates the movements of both the human and the seat in the rear-end impact testing, and the degree of neck injuries can be evaluated using the proposed model by NIC value.

C. *Effectiveness of an active headrest*

In the simulation, the headrest position is moved against the head position, as x-axis is 0, 10, $\cdots$, 80 [mm], and y-axis is 0, 10, $\cdots$, 80 [mm] (See Fig. 9 (a)). It is note that, the other parameters in this simulation were same as in the previous simulation.

Figures 9 (b) and (c) show the data maps of the maximum NIC value, with and without an active headrest mechanism, respectively. A white circle indicates the maximum NIC value obtained at the simulation, and the data between the white circles is calculated by cubic interpolation based on a Delaunay triangulation.

The maximum NIC values of all headrest position decrease to about 60.9 % in average at the seat with an active headrest, and the standard deviation is about 14.5 %. It can be confirmed that the active headrest is effective for reducing neck injuries. In this manner, the proposed simulator can assist for designing

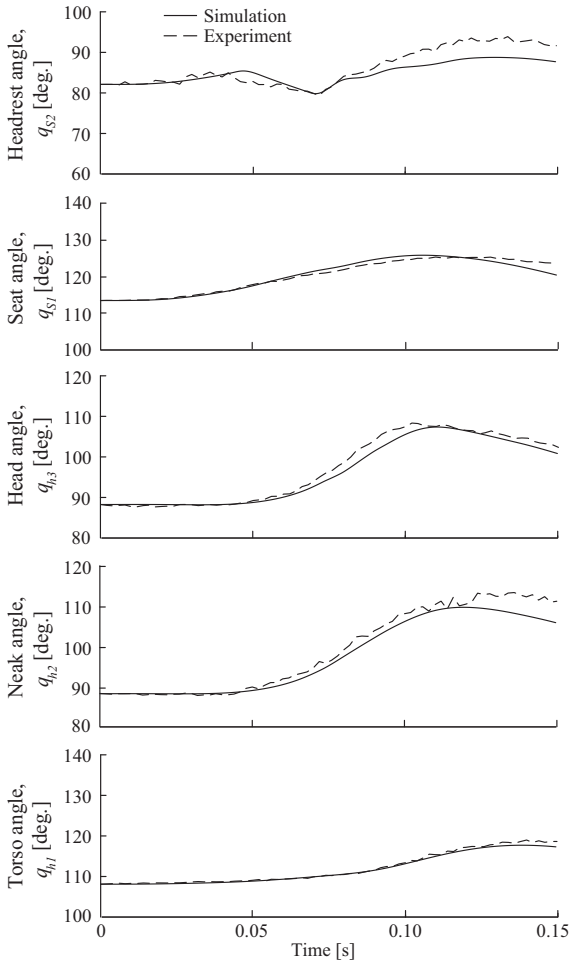

Fig. 7. Comparison of the experimental and simulated results of joint angle.

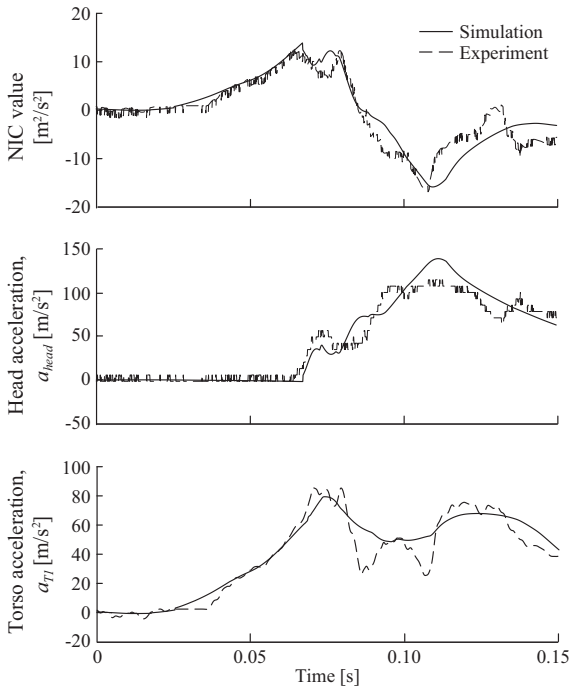

Fig. 8. Comparison of the experimental and simulated results of NIC and accelerations.

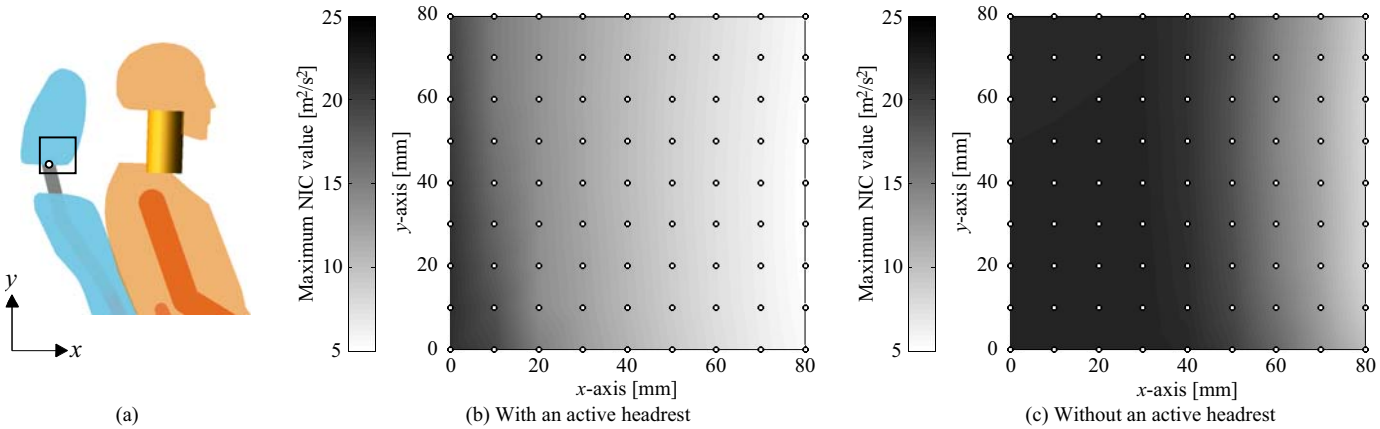

(a) (b) With an active headrest (c) Without an active headrest

Fig. 9. The maximum NIC value with/without an active headrest according to the headrest position.

an effective driving seat reducing neck injuries.

IV. Conclusion

In this paper, the model for analyzing neck injuries based on mechanical impedance was constructed. The model with the active headrest mechanism, which is developed to reduce neck injuries, enabled to recreate movements of a human and a seat in the rear-end impact testing to some extent. The simulation experiments indicated that the active headrest mechanism is effective for reducing neck injuries.

Future research will be more coordinated to correspond to behavior between the human-seat model and the dummy in the rear-end impact testing. Furthermore, it will be analyzed the relationship between human body size and neck injury degrees, and a new mechanism will be designed for reducing neck injuries.

References

[1] National Police Agency : "Situation of the occurrence of traffic accident in 2008," 2009 (in Japanese).

[2] The General Insurance Association of Japan : "The actual condition of traffic accidents of seeing to automobile insurance data (April 2001 ~ March 2002)," 2003 (in Japanese).

[3] M. Y. Svensson, B. Aldman, H. A. Hansson, P. Lövsund, T. Seeman, A. Sunesson, T. Örtengren : "Pressure effects in the spinal canal during whiplash extension motion - A possible cause of injury to the cervical spinal ganglia," *Proceedings of International IRCOBI Conference on the Biomechanics of Impacts*, pp.189-200, 1993.

[4] O. Boström, M. Y. Svensson, B. Aldman, H. A. Hansson, Y. Haland, P. Lövsund, T. Seeman, A. Suneson, A. Säljö, T. Örtengren : "A new neck injury criterion candidate based on injury findings in the cervical spinal ganglia after experimental neck extension trauma," *Proceedings of International IRCOBI Conference on the Biomechanics of Impacts*, pp.123-136, 1996.

[5] K. -U. Schmitt, M. H. Muser, P. Niederer : "A new neck injury criterion candidate for rear-end collisions taking into account shear forces and bending moments," *Proceedings of the 17th International Technical Conference on the Enhanced Safety of Vehicles*, Report No.184, 2001.

[6] M. Y. Svensson, P. Lövsund, Y. Haland, S. Larsson : "The influence of seat-back and head-restraint properties on the head-neck motion during rear-impact," *Proceedings of International IRCOBI Conference on the Biomechanics of Impacts*, pp.395-406, 1993.

[7] G. Nilson : "Effects of seat and seat-belt design on car occupant response in frontal and rear impacts," *Doctoral thesis, Department of Injury Prevention, Chalmers University of Technology*, S-412 96 Göteborg, Sweden, 1994.

[8] K. Furusu : "Analysis of injury of human cervical spine using finite element method," *The R & D Review of Toyota CRDL*, Vol.33, No.1, pp.53-61, 1998 (in Japanese).

[9] S. W. Kirkpatrick, R. MacNeill, R. T. Bocchieri : "Development of an LS-DYNA occupant model for use in crash analyses of roadside safety features," *Proceeding of the 82nd Annual Meeting of the Transportation Research Board(CD-ROM)*, Paper No. 03-4450, 2002.

[10] S-C. Huang : "Analysis of human body dynamics in simulated rear-end impacts," *Human Movement Science*, Vol.17, pp.821-838, 1998.

[11] S-C. Huang, R. L. Huston : "Influence of the head restraint position on dynamic response of the head/neck system under whiplash loading," *Biomedical Engineering, Applications, Basis and Communications*, Vol.15, No.4, pp.164-169, 2003.

[12] Y. Takeda, Y. Tanaka, T. Tsuji, T. Takeshima, T. Kusuhara, Y. Kawashima : "A neck injury analyzer tool based on mechanical impedance characteristics for the design of human-seat systems," *Proceedings of IEEE International Conference on Robotics and Biomimetics*, pp.130-135, 2004.

[13] K. Kishida : "Dynamics of solids," *Baifukan*, 1993 (in Japanese).

[14] DELTA KOGYO CO.,LTD., Seat for vehicle, Japanese Published Patent Application 2005-132345, 2005 (in Japanese).

[15] T. Irie, H. Ola, T. Yamamoto : "Measurement of biomechanical properties on skin by impact response," *IEICE Transactions on Information and Systems D-II*, Vol.75, No.4, pp.799-807, 1992 (in Japanese).

[16] G. A. Gabriele, K. M. Ragsdell : "The generalized reduced gradient method: a reliable tool for optimal design," *Transactions of the ASME, Journal of Engineering Industry*, 99, pp.394-400, 1977.